J Digit Imaging (2015) 28:755–760
DOI 10.1007/s10278-015-9789-1

Comparison of Two Deformable Registration Algorithms in the Presence of Radiologic Change Between Serial Lung CT Scans

Alexandra R. Cunliffe[1] · Bradley White[1] · Julia Justusson[1] · Christopher Straus[1] · Renuka Malik[2] · Hania A. Al-Hallaq[2] · Samuel G. Armato III[1]

Published online: 31 March 2015

Abstract We evaluated the image registration accuracy achieved using two deformable registration algorithms when radiation-induced normal tissue changes were present between serial computed tomography (CT) scans. Two thoracic CT scans were collected for each of 24 patients who underwent radiation therapy (RT) treatment for lung cancer, eight of whom experienced radiologically evident normal tissue damage between pre- and post-RT scan acquisition. For each patient, 100 landmark point pairs were manually placed in anatomically corresponding locations between each pre- and post-RT scan. Each post-RT scan was then registered to the pre-RT scan using (1) the Plastimatch demons algorithm and (2) the Fraunhofer MEVIS algorithm. The registration accuracy for each scan pair was evaluated by comparing the distance between landmark points that were manually placed in the post-RT scans and points that were automatically mapped from pre- to post-RT scans using the displacement vector fields output by the two registration algorithms. For both algorithms, the registration accuracy was significantly decreased when normal tissue damage was present in the post-RT scan. Using the Plastimatch algorithm, registration accuracy was 2.4 mm, on average, in the absence of radiation-induced damage and 4.6 mm, on average, in the presence of damage. When the Fraunhofer MEVIS algorithm was instead used, registration errors decreased to 1.3 mm, on average, in the absence of damage and 2.5 mm, on average, when damage was present. This work demonstrated that the presence of lung tissue changes introduced following RT treatment for lung cancer can significantly decrease the registration accuracy achieved using deformable registration.

Keywords Chest CT · Image registration · Lung · Radiotherapy

Introduction

For patients who undergo radiation therapy (RT) for lung cancer treatment, computed tomography (CT) scans are acquired regularly to assess changes in tumor size and normal tissue reaction to treatment. Comparison of lung CT images over time is complicated by differences in patient positioning and respiratory phase between scans. Deformable image registration may thus be used to identify spatially corresponding locations between scans despite these differences. Several deformable registration algorithms have demonstrated success in lung CT scan co-registration, with a high degree of registration accuracy (e.g., <1 mm average registration error) between scans [1, 2]. Past experience with the Plastimatch demons deformable registration algorithm [3] showed that average registration errors of less than 0.5 mm were present between co-registered serial CT scans derived from healthy patients [4]. For these studies, however, only physical changes such as differences in respiratory phase or technical image acquisition parameters existed between scans. The registration process is further complicated when pathologic changes between serial scans are also present, potentially leading to lower registration accuracy. For example, Palma et al. [5] observed average registration errors >4 mm when they used B-spline

This work was presented, in part, as an oral presentation at the SIIM 2014 Annual Meeting, Long Beach, CA (2014).

✉ Samuel G. Armato, III
s-armato@uchicago.edu

[1] Department of Radiology, The University of Chicago, 5841 S. Maryland Ave., MC 2026, Chicago, IL 60637, USA

[2] Department of Radiation & Cellular Oncology, The University of Chicago, 5758 S. Maryland Ave., Chicago, IL 60637, USA

registration to register post-RT lung CT scans containing fibrotic changes with scans acquired before RT.

This study evaluated the registration accuracy of pre- and post-RT thoracic CT scans for lung cancer patients. Specifically, the registration accuracy achieved when normal lung tissue damage exists in post-RT scans was compared with the accuracy achieved in the absence of changes between scans. Two deformable image registration algorithms (Plastimatch v. 1.5.12-beta demons and Fraunhofer MEVIS v. 1.1 Fast CT lung registration [6]) were investigated. The hypothesis of this study was that both algorithms would exhibit reduced registration accuracy when radiologic abnormalities developed due to the increased complexity of the registration task.

Materials and Methods

Patient Database

Twenty-five patients who underwent curative-intent RT for lung cancer at The University of Chicago Medicine between January 2007 and September 2011 were retrospectively identified under IRB approval. All patients received curative levels of radiation dose (≥60 Gy) delivered using 6 MV or 6 and 18 MV photon beams while immobilized using custom alpha cradles. Treatment planning was performed under the supervision of a radiation oncologist, with dose calculations corrected for heterogenous tissue density. For each patient, two diagnostic quality thoracic CT scans acquired (1) less than 6 months before RT and (2) less than 12 weeks following RT were collected. Additionally, each patient's RT treatment planning CT scan with an associated dose map calculated in Pinnacle® 7.6, 8.0, or 9.0 (Philips Systems, Andover, MA) was collected. Dose maps were aligned with planning scans using tri-linear interpolation in CERR v. 4.0 Beta [7]. For all scans, semi-automated lung segmentation was performed by an experienced thoracic researcher (AC) using Pinnacle® 9.0 model-based segmentation. One patient was eliminated from the study due to poor scan quality degraded by motion and large differences in patient positioning between scans that prevented accurate evaluation of registration accuracy. Patient demographic information and technical imaging parameters for the remaining 24 patients are summarized in Table 1.

Table 1 Patient demographic information, treatment details, and CT scan parameters

Number of patients	24 Male (n=9) Female (n=15)
Median patient age (range) [year]	66 (47–82)
Number with smoking history	23
Lung cancer histology	NSCLC (n=17) SCLC (n=7)
Tumor location	Upper (n=18) Middle (n=2) Lower (n=4)
Treatment regimen:	Concurrent chemo-RT (n=19) Sequential chemo-RT (n=3) RT only (n=2)
Treatment type	IMRT (n=3) 3D-CRT (n=21)
Median radiation dose (range) [Gy]	66 (60–70)
Dose per fraction [Gy]	2 (n=23) 2.5 (n=1)
Motion management	Gated (n=16) Free breathing (n=8)
Mean PTV volume (range) [cc]	554 (90–1276)
Median time between pre-RT scan and RT start (range) [days]	18 (4–75)
Median time between RT end and post-RT scan (range) [days]	32 (2–82)
Diagnostic scan parameters (n=48):	
Scanner type	Philips Brilliance 16 (n=8) Philips Brilliance 16P (n=21) Philips Brilliance 64 (n=19)
Peak kilovoltage [kVp]	120 (n=42) 140 (n=6)
Slice thickness/spacing [mm]	1.0
Mean exposure (range) [mAs]	235 (124–381)
Mean pixel spacing (range) [mm]	0.66 (0.51–0.83)
Mean pixel spacing difference between paired scans (range) [mm]	0.05 (0–0.18)

CT Scan Assessment of Radiologic Change

An attending radiologist with over 10 years of experience (CS) compared each of the post-RT scans with the corresponding pre-RT scan for the presence of mild, moderate, or severe normal lung tissue abnormalities that had developed following RT (Fig. 1) [8]. Analysis was constrained to 60 32×32-pixel (approximately 2×2 cm) regions of interest (ROIs) that were automatically placed within the normal lung tissue of each post-RT scan. Specifically, these ROIs were randomly placed within each of four dose regions (<10, 10–30, 31–50, and >50 Gy) of the lungs in the treatment planning scan dose map and were prevented from overlapping with the planned target volume (PTV). This process ensured that ROIs captured normal tissue damage rather than residual tumor. To associate ROIs in the planning scan dose map with the post-RT scan, each patient's treatment planning CT scan (and thus, the associated dose map) was automatically registered to their post-RT scan using the Plastimatch deformable registration algorithm [9]. Following radiologist review of all ROIs in all scans, patients were identified as having normal tissue abnormalities in the post-RT scan if at least one ROI had been categorized by

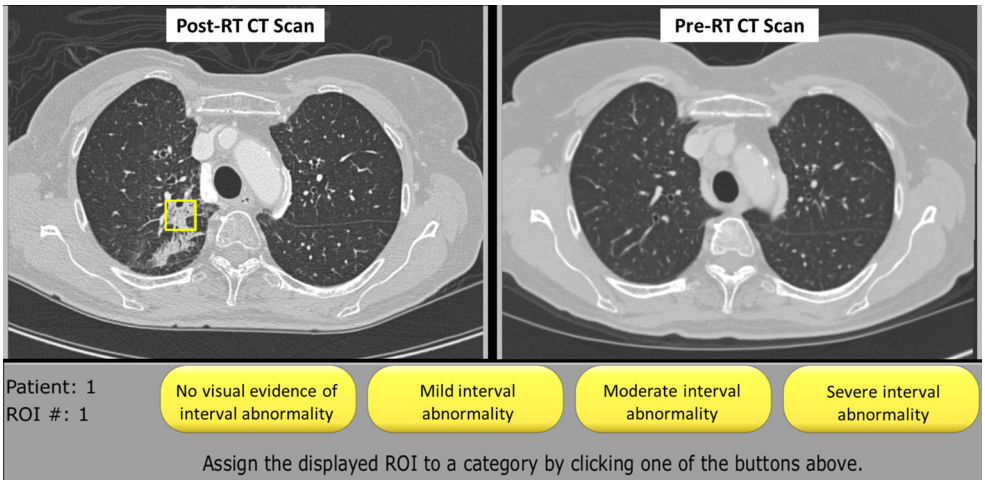

Fig. 1 Randomly selected ROIs (*yellow box*) in each patient's post-RT scan (*left*) were compared with the pre-RT scan and categorized as containing no, mild, moderate, or severe interval abnormality

the radiologist as containing moderate or severe interval abnormalities.

Manual Landmark Matching

A set of 100 landmark points was automatically identified in the lungs of each pre-RT scan. The algorithm used to select these landmarks (iX v.1.2.0.0) [10] ensured that points (1) were located in high pixel-value-gradient regions and (2) were evenly distributed throughout the lungs. Points were also prevented from overlapping with the tumor as defined by the PTV in the planning scan, which had been registered to the pre-RT scan using affine registration. PTVs were excluded from the landmark matching process because large degrees of tumor shrinkage in the post-RT scan limit the ability to accurately identify matched landmark points manually within the PTV. Two researchers (JJ and BW) who received previous training in thoracic anatomy and landmark matching manually identified matched landmark points in each patient's post-RT scan that corresponded with the identified landmarks in the patient's pre-RT scan. If a matched landmark point could not be confidently identified in the post-RT scan, it was not included for further analysis. All matched landmark points were reviewed and edited if necessary by an experienced thoracic researcher (AC).

Automated Landmark Matching

To obtain point-to-point anatomic comparison between pre- and post-RT scans, each patient's post-RT CT scan was registered to the pre-RT scan using both the Plastimatch and the Fraunhofer MEVIS Fast deformable registration algorithms. For both algorithms, registration proceeded as a multi-stage process, with registration at low resolution and using simple transformations occurring before high-resolution stages with additional degrees of freedom in image motion. Parameters used for registration with the Fraunhofer MEVIS algorithm were optimized by the developers for fast, accurate deformable registration using the publically available DIR-Lab dataset [11, 12]. The registration parameters used for demons registration with Plastimatch (Table 2) were selected because they demonstrated high registration accuracy in an independent patient database consisting of healthy thoracic diagnostic CT scans.[1] Based on the displacement vector field output by each algorithm, the identified landmarks in each pre-RT scan were automatically mapped to the corresponding location in the post-RT scan. For both algorithms, the Euclidean distance between manually and automatically identified matched landmark points in the post-RT scan (d_E) was calculated (Fig. 2). Regression modeling was used to model d_E as a function of the registration algorithm (Algorithm_j where $j \in \{1,2\}$) and whether radiologic changes were present ($\text{Presence of Change}_k$ where $k \in \{1,2\}$), while accounting for random patient-specific differences in d_E (Patient_i where $i \in \{1,2,\ldots, 24\}$), according to the following formula:

$$\{d_E\}_{ijkl} = \text{Patient}_i + \text{Algorithm}_j + \text{Presence of Change}_k + \epsilon_{ijkl}$$

where ϵ_{ijkl} represents the residual error in the model fit. Analysis of variance (ANOVA) was then performed to determine whether the registration algorithm and/or the presence of radiologic change significantly ($p<0.05$) impacted d_E.

Results

Between 66 and 93 (median 85), matched landmark points were manually identified for each patient, for a total of 1977 points. The point location was edited by the experienced thoracic researcher for 2–29 (median 15) points per patient. The radiologist identified eight patients as having radiologic evidence of normal lung tissue damage in their post-RT scan,

Table 2 Parameters for multi-stage demons deformable registration using Plastimatch

Stage	Transformation	Subsampling scaling factor in [x, y, z]	Smoothing kernel standard deviation (mm)	Filter width in [x, y, z]	Image homogenization
1	Translation	[10 10 5]	–	–	–
2	Translation	[4 4 2]	–	–	–
3	Affine	[4 4 2]	–	–	–
4	Demons	[4 4 2]	1	[3 3 5]	2
5	Demons	[2 2 1]	0.8	[3 3 5]	1
6	Demons	[1 1 1]	0.6	[3 3 5]	1

with between 1 and 31 (median 3) ROIs per patient identified as containing moderate or severe abnormalities. For both algorithms, average d_E across patients was smaller in the absence of abnormalities (Table 3). Seven of the eight patients with abnormalities had smaller average d_E using the Fraunhofer MEVIS algorithm than using the Plastimatch algorithm, compared with 11 of the 16 patients without abnormalities (Fig. 3). Regression modeling showed that d_E increased significantly ($p<0.05$) due to the presence of abnormalities and the use of the Plastimatch algorithm.

Discussion

This study demonstrated that radiologic changes between lung CT scans have a significant effect on the registration accuracy of deformable registration. Both the Plastimatch and Fraunhofer MEVIS algorithms demonstrated inferior CT scan alignment accuracy in the presence of interval normal lung tissue abnormalities. While the presence of abnormalities increased the registration error by 2.2 mm, on average, using the Plastimatch algorithm, average registration error was increased by 1.2 mm using the Fraunhofer MEVIS algorithm (Table 3). The superior registration accuracy observed using the Fraunhofer MEVIS algorithm may be due to the fact that this algorithm is highly constrained to prevent overfitting through unrealistic deformations. For example, one of the parameters in the objective function used to determine the deformation penalizes for highly curved displacement vectors, which represent unrealistic deformations. These constraints are especially important when structural changes exist between scans, complicating the registration process. The parameters used for registration with the Plastimatch and Fraunhofer MEVIS algorithms were selected due to the high registration accuracy achieved in independent databases; it is possible, however, that an alternative choice of parameters (or even a unique set of parameters for each patient) may be more appropriate for use with the current database, resulting in further improvements in the accuracy of image registration.

Some potential weaknesses may impact the findings of this study. First, manual identification of matched landmark points in the post-RT scans could have resulted in incorrect placement of some points. Furthermore, because the landmark matching task was divided between two researchers, differences in the accuracy of point placement may exist between the researchers. These errors were reduced in several ways. First, prior to beginning the study, the researchers received training on a common test case; no significant difference in the placement of matched landmark points was observed between the two researchers. Second, during landmark matching, all points were visualized using all three planar views, facilitating easy comparison between regions in pre- and post-RT scans (Fig. 4). Third, all manually placed matched landmark points were reviewed by a third researcher (AC), thus preserving consistency among scans annotated by the two researchers.

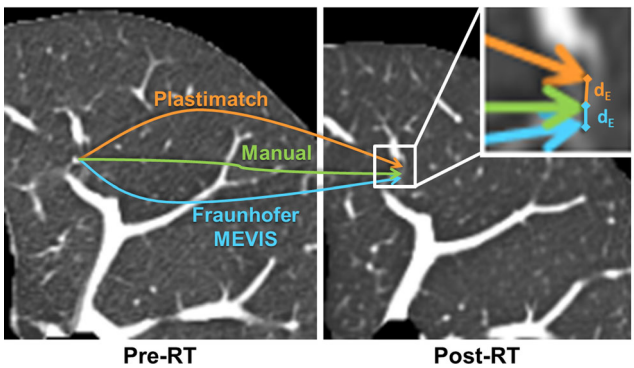

Fig. 2 Method used to calculate the Euclidean distance between manually and automatically placed matched landmark points (d_E) in a post-RT scan

Table 3 Average Euclidean distance (d_E) between manually and automatically identified matched landmark points

	Registration accuracy (range) [mm]	
	Plastimatch	Fraunhofer MEVIS fast
Abnormalities present	4.6 (1.3–10.1)	2.5 (1.3–4.9)
Abnormalities absent	2.4 (0.7–6.9)	1.3 (0.9–2.8)

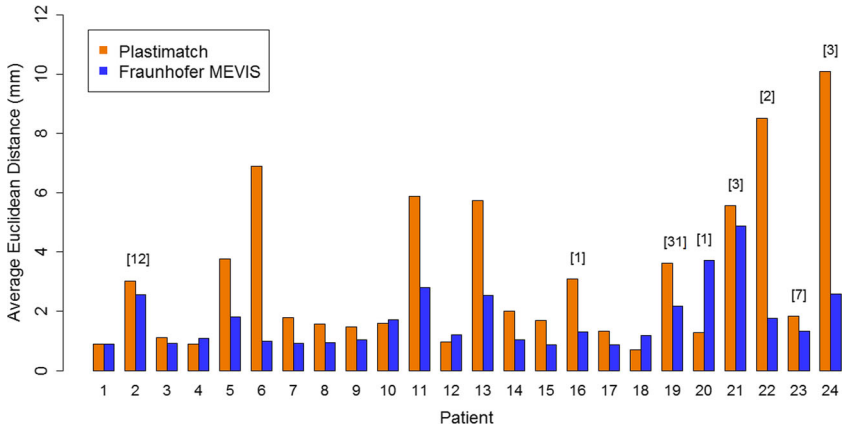

Fig. 3 Average Euclidean distance (d_E) between manually and automatically identified matched landmark points for each patient. Shown in *brackets*: number of ROIs categorized as containing moderate or severe changes

Although the majority of patients with larger registration errors using Plastimatch had abnormalities in their post-RT scans, there were some patients who exhibited large registration errors despite the absence of radiologist-identified abnormalities within the 60 ROIs. If the selected ROIs did not overlap with regions containing damage, our methods would fail to identify some patients with abnormalities. Thirty of the 60 ROIs in each scan were placed in high-dose (≥30 Gy) regions where normal tissue damage was most likely to be observed [13, 14]. It is thus unlikely that normal tissue damage in these regions went uncategorized due to the small volume (15 % of total lung volume on average) of these dose regions. Furthermore, this method of classifying radiation damage allowed the radiologist to examine changes on a small regional basis, facilitating careful classification of both subtle and obvious radiation-induced damage. Large registration errors in the absence of abnormalities are also unlikely due to differences in patient positioning or scan appearance, as all CT scans were acquired on Philips CT scanners with 1-mm slice thickness and sub-millimeter pixel spacing (Table 1) and were reconstructed using identical lung convolution and lung smoothing kernels. During scan acquisition, all patients were supine with arms raised above the head, and patients were instructed to inspire and hold their breath. Instead, registration errors when abnormalities were absent may be due to notable patient improvement between pre- and post-RT scans. For example, patients #5 and #6 experienced a substantial decrease in tumor size following RT and patient #11 experienced lung volume expansion, which may explain the low registration accuracy achieved using Plastimatch (Fig. 3). Future studies should aim to characterize the degree of improvement following RT (e.g., decrease in lesion size) and the subsequent effects on registration accuracy.

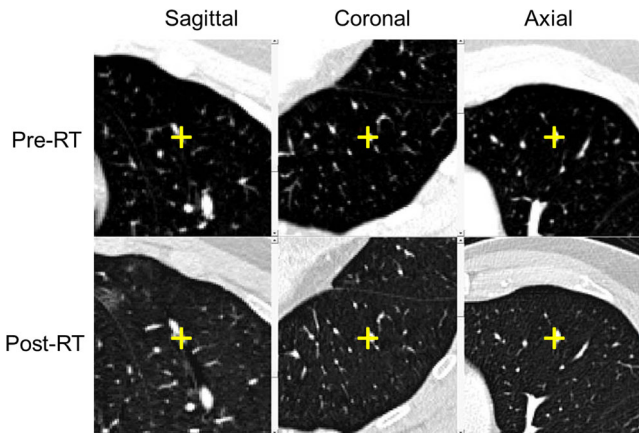

Fig. 4 Display used in iX v.1.2.0.0 for manual placement of matched landmark points in each post-RT scan

While the Fraunhofer MEVIS algorithm was well suited for CT scan co-registration in the presence of normal lung tissue changes, future studies should investigate whether successful registration can be performed in the presence of other changes that can occur during lung cancer treatment. Additional treatments that may alter the visual appearance of the lungs on CT scans include chemotherapy and surgery. While the focus of the current study was to evaluate the accuracy with which normal lung tissue could be registered between CT scans acquired before and after RT, future studies are needed to determine the accuracy of deformable registration in tumorous portions of the lung where large degrees of tumor shrinkage are often present. Accurate registration of tumor tissue could allow for planned RT dose to the target volume to be mapped from treatment planning to diagnostic scans. The current study focused exclusively on normal lung tissue deformable registration because of its potential future utility to evaluate radiation-induced normal lung tissue damage. Specifically, regions of pre- and post-RT diagnostic CT scans that have been identified through registration could be compared quantitatively to evaluate changes following radiation delivery. Patients can also develop chronic fibrotic changes that may differ from the acute normal tissue damage investigated here. Additional studies would be needed to determine whether deformable registration could be used throughout the entire course of lung cancer treatment to assess regional changes between serial scans.

Conclusions

The accuracy of two registration algorithms was evaluated in the presence of normal lung tissue changes that had developed between pre- and post-RT CT scans. Both algorithms experienced decreased registration accuracy when changes were present, with the Fraunhofer MEVIS Fast algorithm demonstrating significantly improved registration accuracy compared with the Plastimatch algorithm. Deformable registration could be used in future studies to identify corresponding anatomic locations between serial CT scans, thus facilitating evaluation of image-based change in normal lung tissue following RT.

Acknowledgments Supported, in part, by NSF REU Award No. 1062909 and NIH Grant Nos. S10 RR021039, P30 CA14599, and T32 EB002103. Anonymized, compliant images were provided by The Human Imaging Research Office (HIRO), which is supported in part by pilot research funding provided by the Virginia and D.K. Ludwig Fund for Cancer Research through the Imaging Research Institute in the Biological Sciences Division of The University of Chicago.

References

1. Murphy K, van Ginneken B, Reinhardt JM, Kabus S, Ding K, Deng X, Cao K, Du K, Christensen GE, Garcia V, Vercauteren T, Ayache N, Commowick O, Malandain G, Glocker B, Paragios N, Navab N, Gorbunova V, Sporring J, de Bruijne M, Han X, Heinrich MP, Schnabel JA, Jenkinson M, Lorenz C, Modat M, McClelland JR, Ourselin S, Muenzing SE, Viergever MA, De Nigris D, Collins DL, Arbel T, Peroni M, Li R, Sharp GC, Schmidt-Richberg A, Ehrhardt J, Werner R, Smeets D, Loeckx D, Song G, Tustison N, Avants B, Gee JC, Staring M, Klein S, Stoel BC, Urschler M, Werlberger M, Vandemeulebroucke J, Rit S, Sarrut D, Pluim JP: Evaluation of registration methods on thoracic CT: The EMPIRE10 challenge. IEEE Trans Med Imaging 30:1901–1920, 2011
2. Brock K: Results of a multi-institution deformable registration accuracy study (MIDRAS). Int J Radiat Oncol Biol Phys 76:583–596, 2010
3. Sharp G, Kandasamy N, Singh H, Folkert M: GPU-based streaming architectures for fast cone-beam CT image reconstruction and demons deformable registration. Phys Med Biol 52:5771–5783, 2007
4. Cunliffe A, Al-Hallaq H, Labby Z, Pelizzari C, Straus C, Sensakovic W, Ludwig M, Armato S: Lung texture in serial thoracic CT scans: assessment of change introduced by image registration. Med Phys 8:4679–4690, 2012
5. Palma DA, Van Sörnsen de Koste J, Verbakel WFAR, Senan S: A new approach to quantifying lung damage after stereotactic body radiation therapy. Acta Oncol 50:509–517, 2011
6. Rühaak J, Heldmann S, Kipshagen T, Fischer B: Highly accurate fast lung CT registration. Proc SPIE 8669:86690Y–86690Y–9, 2013
7. Deasy JO, Blanco AI, Clark VH: CERR: A computational environment for radiotherapy research. Med Phys 30:979–985, 2003
8. Cunliffe AR, Armato SG, Straus C, Malik R, Al-Hallaq HA: Lung texture in serial thoracic CT scans: correlation with radiologist-defined severity of acute changes following radiation therapy. Phys Med Biol 59: 5387–5398, 2014
9. Cunliffe AR, Armato SG, Fei XM, Tuohy RE, Al-Hallaq HA: Lung texture in serial thoracic CT scans: registration-based methods to compare anatomically matched regions. Med Phys 40: 061906–1–061906–9, 2013
10. Murphy K, van Ginneken B, Klein S, Staring M, de Hoop BJ, Viergever MA, Pluim JPW: Semi-automatic construction of reference standards for evaluation of image registration. Med Img Anal 15:71–84, 2011
11. Castillo R, Castillo E, Guerra R, Johnson VE, McPhail T, Garg AK, Guerrero T: A framework for evaluation of deformable image registration spatial accuracy using large landmark point sets. Phys Med Biol 54:1849–1870, 2009
12. Castillo R, Castillo E, Martinez J, Shenoy M, Guerrero T: Four-dimensional deformable image registration using trajectory modeling. Phys Med Biol 5:305–327, 2009
13. Movasas B, Raffin TA, Epstein AH, Link CJ: Pulmonary radiation injury. Chest 111:1061–1076, 1997
14. Jenkins P, Welsch A: Computed tomography appearance of early radiation injury to the lung: Correlation with clinical and dosimetric factors. Int J Radiat Oncol Biol Phys 54:329–339, 2002